Translated from *Uspekhi Khimii* **60** 2065–2088 (1991) U.D.C. 539.19:541.57

Compounds of the *f*-elements. Chemical bonding and electronic structure

Z M Sabirov, A A Bagatur'yants
Institute of Chemistry, Bashkir Scientific Centre, Ural Branch of the USSR Academy of Sciences, Ufa
Institute of Chemical Physics, USSR Academy of Sciences, Moscow

ABSTRACT. **Recent data from experimental and theoretical studies of the nature of the chemical bonding in *f*-element compounds and their electronic structure are reviewed. Implicit and explicit methods of accounting for relativistic effects in quantum-chemical calculations are briefly examined. Results of quantum-chemical calculations of lanthanide trihalides, lanthanide and actinide cyclopentadienides, and other *f*-element compounds are analysed. Questions about the electronic and geometric structure, the nature of the π- and σ-bonding, and the role of *d*- and *f*-orbitals in forming chemical bonds are discussed.**

The bibliography includes 95 references.

Contents

I.	Introduction	1059
II.	Relativistic quantum chemistry	1060
III.	Lanthanide trihalides	1061
IV.	Lanthanide and actinide cyclopentadienide derivatives	1063
V.	Other *f*-element compounds	1068

I. Introduction

In the lanthanide (Ce → Lu) and actinide (Th → Lr) series, electrons are placed successively in the 4*f*- and 5*f*-orbitals respectively. Therefore, lanthanides (Lns) and actinides (Ans) are frequently classified together as *f*-elements. The varied and ever expanding application of *f*-element compounds in science and technology has in the last decade stimulated interest in the study of their electronic structure and the nature of their chemical bonding.

Crystal field theory[1,2] has been widely used in the majority of earlier theoretical studies for analysing the electronic structure of Lns and Ans. The reason for this is that the *f*-electrons have features different from those for electrons in other subshells. Thus, the energy levles of the 4*f*-orbitals in Lns are rather close to those of the 5*s*-, 5*p*- and 5*d*-orbitals. However, the 4*f*-states extend little into space and the electrons in them are to a large extent localised inside the 5*s*- and 5*p*-subshells.[3] As a result, 4*f*-orbitals poorly overlap with orbitals of neighbouring atoms and the bonding in Lns is mainly due to 5*s*- and 5*p*-electrons, i.e., it is nearly purely ionic. Analogous arguments for the role of the *f*-electrons were made for actinide compounds.

However, the majority of recent studies on the electronic structure of *f*-compounds have utilised molecular-orbital (MO) methods owing to the obvious limitation of crystal field theory for describing *f*-compounds.[3] Such an approach significantly facilitates development of general concepts about the chemical bonding in compounds with *f*-electrons. Previous reports[3–8] are recommended for familiarising oneself with the current state of affairs in this area. Moreover, these references contain numerous citations to earlier reviews and reports on the respective topics.

Hence, the capabilities of quantum-chemical cluster models and methods of describing various characteristics of the electronic structure of solids based on the *f*-elements have been explored.[3,4] In these studies, special attention was paid to the orderly statement of the basic principles of the cluster approach for modelling the electronic structure of solids and the quantum-chemical approaches used in cluster calculations. The nature of interatomic interactions and the role of *f*-subshells in chemical bonding were analysed in detail.

Quantum-chemical calculations of atoms, ions and actinide molecules have been generalised and systematised in a monograph.[5] Features of the electronic structure of 5*f*-elements, the stability of the different An oxidation states, and the analogy between Lns and Ans were analysed. Isomer shifts in Mössbauer spectra were interpreted. The relative role of various mechanisms in forming chemical bonds and the influence of relativistic effects on the properties of Lns and Ans were the subjects of much attention.

The periodic (tetrad) regularity in the change of many properties of the free atoms and ions of the *f*-elements (ionisation potential, electron affinity, redox potentials, etc.) have been analysed.[6]

Relativistic effects in structural chemistry have been reviewed.[7,8] These reviews contain the most detailed information on this subject. A short but rather complete analysis of the relativistic methods of quantum chemistry that are used for calculating the electronic structure of compounds containing heavy elements is also provided.

However, it is noteworthy that few studies analyse the electronic structure of *f*-compounds within the framework of MO methods. Calculations for rather large molecular systems of interest to chemists are just beginning. Consequently, fundamental questions about the features and details of the electronic structure (participation of various groups of electrons in the chemical bonding, specific role of *f*-subshells, relation of the reactivity of *f*-compounds to their electronic structure, etc.) are far from finally resolved.

In the present review, recent results are reviewed and analysed. These have not appeared previously in monographs and reviews and are mainly theoretical studies of the fundamental chemical properties of *f*-element organometallic compounds: their electronic and geometric structure and their reactivity.

Results are also presented for calculations of the electronic and geometric structure of lanthanide trihalides (LnX_3). This material is placed in a separate section since LnX_3 have been a test case of the *f*-block for verifying the capabilities of many quantum-chemical methods.

Methodical problems related to the study of the electronic structure of the *f*-elements should also be noted. As the atomic number of an element increases (nuclear charge Z), the total and

kinetic energy of the electrons increases. For heavy elements, in particular the Lns and even more the Ans, relativistic corrections become important [these are of the order of $(v/c)^2$, where v is the velocity of the electrons and c is the speed of light]. Therefore, the role of relativistic effects and explicit and implicit methods of accounting for them in quantum-chemical calculations must be discussed, although briefly.

II. Relativistic quantum chemistry

The majority of quantum-chemical calculations of interest to chemists are based on the solution of the nonrelativistic Schrödinger equation, the Hamiltonian of which is constructed assuming that the interaction of electrons does not depend on their velocity. The relativistic dependence of the rest mass of particles on velocity is also ignored. These approximations formally correspond to an infinite speed of light. Such calculations are suitable, for example, for approximating the total energy or wave functions of light atoms or molecules consisting of them. The Schrödinger Hamiltonian is unsuitable for describing the finer details of electronic structure. The special structure of a multi-electron atom cannot be even qualitatively described using a nonrelativistic approximation.[9]

The relativistic analogue of the one-electron Schrödinger equation is the Dirac equation. The principal difference between them is that the dependence of the electron mass on its velocity is considered in the relativistic kinetic energy operator. This produces 4 × 4 matrices in the Hamiltonian instead of the usual scalar operators. The solutions of the Dirac equation are four-component wave functions.

Additional difficulties arise on going to multi-electron atoms and molecules. For instance, a complete (conclusive) relativistic theory of electron–electron interaction does not exist. One of the fundamental difficulties is that particles can be generated or absorbed owing to the equivalency of energy and mass. This can occur every time when energy equal to or greater than the rest energy of these particles is transferred during their interaction.[11] The destruction of particles can be systematically accounted for only within the framework of the quantised field concept whereas quantum field theory has its own difficulties and unsolved problems.

Therefore, relativistic effects are accounted for in the majority of cases using approximate Dirac or Dirac–Breit Hamiltonians.[7,8,12] Electron–electron interaction in the first of these is described by the usual nonrelativistic expression. In the second, a relativistic correction (of the order of α^2, where $\alpha = e^2/hc$ is a fine structure constant) to the two electron-interaction, first obtained by Breit, is considered.

Very complicated and long equations must be solved to account for relativistic effects within the framework of the MO LCAO method owing to the appearance of four-component wave functions. Fortunately, only outer valence electrons participate directly in chemical bond formation in the majority of cases. The so-called quasirelativistic approximation is entirely applicable to these. Relativistic effects in this approximation are accounted for to the accuracy given by the $(v/c)^2$ terms.[13]

It is convenient to transform the relativistic Hamiltonian of the multi-electron atom to a form where its nonrelativistic part is clearly separated in order to follow in more detail the relative role and physical meaning of relativistic effects.[14,15] After such a transformation using the Pauli approximation (accounting for terms up to α^2) and in the absence of external magnetic and electric fields, the relativistic Hamiltonian H can be written[8]

$$H = H_0 + H_D + H_{mv} + H_{so},$$

where H_0 is the nonrelativistic Hamiltonian, H_D is the correction for Darwin interaction (the Darwin term has no classical interpretation), H_{mv} is a correction to the kinetic energy accounting for the dependence of particle masses on their velocity, and H_{so} is a correction for spin–orbit coupling.

The correction H_{mv}, which accounts for the dependence of particle masses on their velocity, causes a relativistic contraction of orbitals. This is most noticeable for inner 1*s*- and 2*s*-electrons moving at large velocities.[5,7,8] The inner *p*-orbitals contact to a smaller extent. Owing to the relativistic contraciton of *s*- and *p*-orbitals, electrons in them more effectively screen the nuclear charge. Electrons in *d*- and *f*-orbitals are more weakly attracted to the nucleus. As a result, the *d*- and *f*-orbitals become more diffuse and energetically destabilised (energy levels shift upward relative to their nonrelativistic values).

The correction for spin–orbit coupling H_{so} causes levels to split into sublevels corresponding to different values of total momentum $j = l \pm 1/2$ (l is the orbital moment). Thus, the *p*-level splits into $p_{1/2}$- and $p_{3/2}$-sublevels; the *d*-level, into $d_{3/2}$- and $d_{5/2}$-sublevels, etc.

These relativistic corrections are essential and have a significant influence on the electronic properties of heavy atoms and molecules containing heavy atoms. For example, the lanthanide contraction (decrease of ionic radius on going from La to Lu), which is usually related to incomplete screening of the nuclear charge by 4*f*-electrons, is to a certain degree due to a relativistic effect. A comparison of atomic calculations by Hartree–Fock (nonrelativistic) and Dirac–Fock (relativistic) methods revealed that the lanthanide contraction is 27% due to a relativistic effect.[8,16]

Various quantum-chemical relativistic and quasirelativistic methods for calculating the electronic structure of atomic and molecular systems have been described.[3–5,7,8,16–23] Therefore, we will briefly discuss only those methods that have been used in subsequent studies.

Calculations based on the quasirelativistic or relativistic extended Hückel and *X*α-scattered wave (*X*α-SW) or *X*α-discrete variational (*X*α-DV) methods have been most widely used.

A local approximation for the exchange-correlation potential is used in the *X*α methods. This produces a one-electron Hartree–Fock–Slater equation.[24] There are two methods for solving this equation, which are reflected in their names: *X*α-DV and *X*α-SW.[25,26] Incorporating relativistic corrections does not significantly change the calculation structure of these methods. Relativistic effects have been accounted for within the framework of the *X*α-DV method.[27,28] Relativistic[29,30] and quasirelativistic[31] *X*α-SW methods have been developed. It is noteworthy that *X*α-methods have been successfully employed to interpret photoelectron spectra.

The Hamiltonian is not examined in an explicit form in the relativistically parametrised extended Hückel method,[32–36] like in the nonrelativistic method. The diagonal matrix elements of the effective one-electron Hamiltonian H_{ii} are usually set equal to the orbital energies that are either estimated from experiment or are taken from Dirac–Fock atomic calculations.[37] The off-diagonal elements H_{ij} are estimated using the standard Wolfsberg–Helmholtz formula.

In the quasirelativistic extended Hückel method,[38,39] the usual (quasirelativistic) atomic functions (*p*-, *d*- and *f*-) are used. These are obtained from relativistic ($f_{7/2}$, $f_{5/2}$, $d_{5/2}$, $d_{3/2}$, $p_{3/2}$ and $p_{1/2}$) functions by using the weighted average of each multiplet. This enables such relativistic effects as the relativistic contraction of atomic *s*- and *p*-orbitals and the increased diffuseness of the *d*- and *f*-orbitals in addition to the average shift of the energy levels to be explicitly accounted for. The spin-orbit splitting of the levels and the difference in diffuseness of the two multiplets of the *p*-, *d*- and *f*-orbitals remain unaccounted for. It is proposed that the last two factors have little effect on such properties as the geometry and reactivity.

The principal merit of the extended Hückel method is the complete accounting for overlap intergrals. This enables wave functions with the correct normalisation to be obtained and exchange repulsion effects of filled shells to be qualitatively correctly described. This is very important in describing the structure of complexes. Drawbacks of the extended Hückel method are connected with the lack of accounting for electron-electron interaction, with approximation of the total energy of all orbital energies, and with problems in constructing a satisfactory approximation for the off-diagonal matrix elements H_{ij}. Therefore, this method was very useful for describing conformational effects and other properties that can be interpreted by orbital-energy correlation diagrams. However, it is in general unsuitable for describing the formation and dissociation of chemical bonds and does not treat electrostatic effects.[40]

Naturally, each of the listed methods has its advantages and shortcomings, enables with a different degree of accuracy calculation of the electronic structure, and considers relativistic effects in calculations. Results of various calculations of gaseous LnX_3 are compared in the following section as an illustration of the capabilities of these methods.

III. Lanthanide trihalides

One of the first studies of the nature of the bonding and geometric features of LnX_3 (in the vapour phase) was carried out using the nonrelativistic extended Hückel method (4*f*-orbitals were not included in the valence basis set).[41] The effect of 4*f*-electrons was considered indirectly in the choice of the empirical parameters (the values of the diagonal elements H_{ii}). The most important result of the calculations was the conclusion that a pyramidal structure for these molecules represents the minimum in total energy. An orbital-correlation analysis demonstrated that such a structure enables the optimum interaction between the metal *d*-orbitals (especially d_{z^2}) and the halide *p*-orbitals. The calculated charge on the metal in LaX_3 is much less than +3: +1.10 for LaF_3, +0.66 for $LaCl_3$, +0.54 for $LaBr_3$, and +0.38 for LaI_3. Therefore, these data suggest that the bond in LaX_3 is not purely ionic even for the fluorides and that the covalency increases down the halogen series (F → I).

The structures of LnX_3 have been analysed by the Wolfsberg–Helmholtz method.[42] This is a variation of the extended Hückel method and includes an additional self-consistency procedure for atomic charges. Low-lying excited states of LnX_3 were studied in this work. The transition energies from *f*- to *d*-levels were estimated. A total of 56 molecules were examined. The results obtained (orbital energies, transition energies, atomic charges, etc.) provided a basis for choosing promising molecules for fabrication of new gas lasers.

The electronic structures of MI_3 (M = La, Gd, Lu)[33] have been calculated by the relativistically parametrised extended Hückel method. The experimental data reveal that MI_3 are polar and that a nonplanar structure (pyramidal) represents the minimum in total energy.

The most detailed and thorough of the electronic structures of LnX_3 has been carried out by Ruscic et al.[43] They studied photoelectron spectra (using He I and He II excitation sources) of $LaCl_3$, $LaBr_3$, $CeBr_3$, $NdBr_3$, $LuBr_3$, LaI_3, CeI_3, NdI_3, ErI_3 and LuI_3. The electronic structure of all compounds was calculated by the relativistic $X\alpha$-DV method. An analysis of the results obtained, taking into account literature data for the photoelectron spectra of Ln fluorides and chlorides in addition to mass spectra, demonstrated that the SCF-$X\alpha$ method correctly reproduces the experimental features of the spectra. Regularities found experimentally in the change of the nature of the bonding, the ionisation potentials, and the valence band widths in both the Lns (La → Lu) and the halides (F → I) are discussed.

It has been found[43] that the ionisation energies of the 4*f*-orbitals of light(early) Lns are less than those of the ligand *p*-orbitals. These energies are comparable for the middle Lns. For the heavy (late) Lns, the energies of the 4*f*-electrons decrease so much that they act like core electrons. Although the ionisation energies of the Ln 4*f*-orbitals for the majority of LnX_3 are very close to those of the halide valence orbitals, nevertheless, the 4*f*-orbitals interact very weakly with the halide orbitals. The reason for this is that the 4*f*-electons of the Lns and the valence electrons of the halides are localised in physically separated regions of the molecule. Therefore, the overlap of the respective orbitals is very poor. The corresponding radii of maximal electron density can be used as a measure of the localisation of the Ln orbitals. For the principal component of the $4f_{7/2}$-orbital, the radial electron density is maximal at $r \sim 0.4$ Å for $La^{+1.5}$ and $r \sim 0.3$ Å for $Lu^{+1.01}$ (r is the distance from the nucleus) whereas the maxima for the $5d_{5/2}$-, $6p_{3/2}$-, and 6*s*-orbitals are reached at r = 1.22, 2.27 and 1.89 Å, respectively. Moreover, the electron density in the 4*f*-states is mainly concentrated in the narrow region between 0.2 and 0.7 Å. Such localisation ensures that the 4*f*-orbitals will have a very low chemical activity.

Theoretical and experimental data indicate that the bonding in LnF_3 is primarily ionic ($Ln^{+2.2}$). A more covalent nature is acquired on going to the chlorides ($Ln^{+1.6}$), bromides ($Ln^{+1.3}$) and iodides ($Ln^{+1.01}$). As already demonstrated above, the reason for the highly ionic bonds in the fluorides is the poor overlap between the halide and metal orbitals. The covalency increases primarily as a result of the involvement of 5*d*-, 6*p*- and 6*s*-orbitals. This is confirmed by an analysis of the corresponding overlap integrals between the orbitals and the outer *p*-orbitals of the halides.

The ground state, only La, Ce, Gd and Lu atoms have the electronic configuration $4f^n5d6s^2$. This corresponds to trivalent Lns in organometallic compounds where on 5*d*- and two 6*s*-electrons participate in the bonding. The electronic configuration of other Ln atoms in the ground state does not include the *d*-level. The energy ΔE must be lost in promoting an electron from the 4*f*- to the 5*d*-level (the $4f^n6s^2 \rightarrow 4f^{n-1}5d6s^2$ transition) and convering these Lns to the trivalent state. Naturally, it is expected (under otherwise equal conditions) that as the energy ΔE that must be lost increases, the energy subsequently gained in bond formation decreases. This is confirmed by the fact that the enthalpy change for atomisation of

LnX_3 and lanthanide monoxides correlates with the energy change of the $4f^n6s^2 \rightarrow 4f^{n-1}5d6s^2$ transition in the Ln series.[43,44]

It has been found[43] that the dissociation energy of La, Ce, Gd and Lu monoxides (i.e., Lns that have a populated *d*-level in the atomic ground state) into the atoms (E_d^*, kcal mole^{-1}) decreases smoothly with increasing atomic number according to the law $E_d^* = 190.6 - 3.75N + 0.094N^2$, where $N = Z$(atomic number) $- 57$. In this instance, the change in lanthanide monoxide dissociation energies along the whole series La → Lu should be described by the equation $E_d(N) = E_d^*(N) - \Delta E(N)$, where $\Delta E(N)$ is the energy of the $4f^n6s^2 \rightarrow 4f^{n-1}5d6s^2$ transition for Ln atoms that do not have a populated 5*d*-level in the ground state. The E_d values calculated in this manner[44] correctly describe the experimentally observed double periodicity in the change of dissociation energy of lanthanide monoxides (Fig. 1).

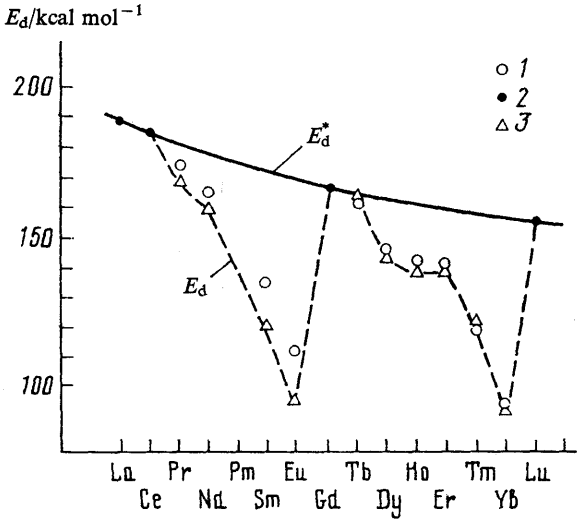


Figure 1. Change of lanthanide monoxide dissociation energy as a function of atomic number.[44] Experimental data (*1*), experimental data used to construct the dependence of E_d^* on N (*2*), calculated E_d (*3*).

The data plotted in Fig. 2[43] demonstrate an analogous periodicity in the change of enthalpy of atomisation for LnX_3.

It is noteworthy that the average bond energy Ln–X (X is a halide) decreases on going from F to I. Hence, the average enthalpy of atomisation of LnF_3, $LnF_3(g) \rightarrow Ln(g) + 3F(g)$, is about 420 kcal mol^{-1}. Consequently, the Ln–F bond energy is 140 kcal mol^{-1}.[43] The corresponding values for $LnCl_3$ are 325 and 108 kcal mol^{-1}; for $LnBr_3$, 290 and 97 kcal mol^{-1}; and for LnI_3, 228 and 76 kcal mol^{-1}.[43] The conclusion is also reached that electrostatic forces provide the principal contributions to the bonding although the positive charges on the Ln ions is always much less than three. This occurs since the overlap integrals between the atomic orbitals of the Lns and halides (which can be viewed as a measure of the covalency) are very small.

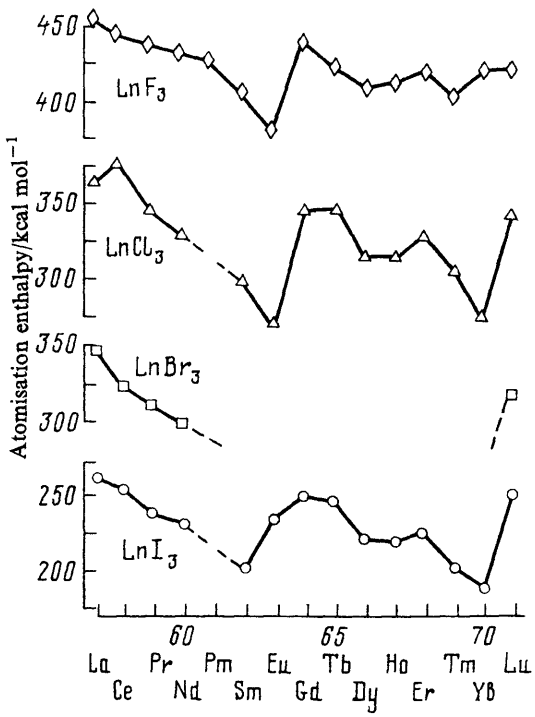


Figure 2. Dissociation enthalpy of LnX_3 into free atoms as a function of Ln atomic number.[43]

Spin-orbit splitting of filled valence and core levels in LnX_3 has been studied.[45] Calculations were made using the relativistically parametrised extended Hückel method. A total of 60 LnX_3 molecules were examined, where X = F → I and Ln = La → Lu. The geometric structure was selected to be the same as in previous studies[43] in order to facilitate comparison with results obtained by the $X\alpha$-DV method. The following basic principles were found. On going from F to I, the positions of the *p*-orbital energy levels of the halides X(*np*) are raised and the width of the valence band (the difference between the highest and lowest energy levels of these orbitals) increases from 1.2 to 2.8 eV. The latter agrees well with photoelectron spectra for La, Gd and Lu trihalides. The width of the X(*ns*)-level band changes from 0.25 to 1.0 eV. The ligand-field splitting of the Ln($5p_{3/2}$)-levels is small [from 0.25 (La) to 0.75 eV (Lu)] compared with the spin-orbit splitting $p_{3/2} - p_{1/2}$, which increases on going from La to Lu from 2.73 to 7.29 eV. On going from F to I and from La to Lu, the splitting of the $5p_{3/2}$-levels decreases. The spin-orbit splitting of the $4f_{7/2}$- and $4f_{5/2}$-levels agrees well with the experimental values obtained for GdX_3 and LuX_3. The charges on the Ln atoms (calculated according to Mulliken) in LnX_3 decrease on going from F to I. The values for LuX_3 are 2.82 (F), 2.37 (Cl), 2.31 (Br) and 2.01 (I). These changes in the charges occur in concert with the decrease of ionisation energy of the 4*f*-electrons and reflect the increasing population of the 6*s*- and 5*d*-orbitals of the Ln. Thus, the orbital charges for LuX_3, where X = F, Cl, Br, and I, are 0.029, 0.156, 0.168 and 0.245 for 6*s*; 0.070, 0.196, 0.220 and 0.326 for $5d_{3/2}$; and 0.090, 0.284, 0.307 and 0.424 for $5d_{5/2}$-orbitals, respectively.

Nonrelativistic nonempirical *ab initio* calculations on LaH_3, LaF_3 and $LaCl_3$ using the program GAUSSIAN-82[45] were also carried out in order to refine further the geometric structures of LnX_3. It was found that the pyramidal C_{3v}-structure is energetically favorable for LaH_3 and LaF_3 whereas the total energy minimum for $LaCl_3$ corresponds to the planar D_{3h}-structure (Table 1).

Table 1. Equilibrium geometric structure parameters of planar (D_{3h}) and pyramidal (C_{3v}) LaX_3.[45]

Molecule	Symmetry	La–X bond length, Å	X–La–X angle, deg	ΔE^*, cm^{-1}
LaH_3	C_{3v}	2.129	114.7	239
	D_{3h}	2.137	120.0	
LaF_3	C_{3v}	2.080	112.0	921
	D_{3h}	2.089	120.0	
$LaCl_3$	C_{3v}	2.613	112.0	−381
	D_{3h}	2.623	120.0	

*$\Delta E = E(D_{3h}) - E(C_{3v})$ is the difference of total energies.

Table 2. Geometric structure and ionisation potential of $LnCl_3$.[47]

Lanthanide (Ln)	Ln–Cl bond length, Å		Cl–Ln–Cl angle, deg		Ionisation potential, eV	
	theory	experiment	theory	experiment	theory	experiment
Ce	2.570	2.569	115.6	111.6	10.0	9.8
Pr	2.566	2.553	108.5	110.8	11.8	10.9–11.2
Nd	2.563	2.545	112.7	–	13.3	12.0
Pm	2.556	–	112.7	–	14.4	–
Sm	2.544	–	113.0	–	15.3	13.7–17.0
Eu	2.532	–	113.2	–	16.4	–
Gd	2.514	2.489	110.0	113.0	17.7	15.5–16.5
Tb	2.496	2.478	109.8	109.9	13.0	13.0–20.5
Dy	2.479	–	110.1	–	14.3	14.0–20.0
Ho	2.464	2.459	112.0	111.2	15.0	15.5–20.0
Er	2.448	–	110.9	–	15.6	11.5–16.0
Tm	2.430	–	108.5	–	15.9	15.3–21.0
Yb	2.421	–	109.6	–	15.9	15.5–21.0
Lu	2.415	2.417	108.2	111.5	18.6	17.4–18.7

The structures of LnX_3 have also been analysed by the INDO method. The electronic structure of LnF_3 has been studied.[46] It was found that the 4*f*-orbitals of Ln atoms have almost no contribution to bond formation. The covalent bonding between Ln and F is mainly due to the Ln 5*d*-, and to a lesser extent, the 6*s*- and 6*p*-orbitals.

Other results[47] demonstrate that the INDO calculations reproduce well the geometric structure and ionisation potentials of LnX_3 (Table 2). The pyramidal structure is energetically favourable (i.e., corresponds to the total energy minimum). It was demonstrated that the *f*-orbitals contribute little to the bonding. Nevertheless, the calculated Ln–Cl bond lengths agree better with the experimental values if the *f*-orbitals are included in the calculations.

Therefore, results of quantum-chemical calculations using various methods suggests, firstly, that the bonding in LnX_3 is purely ionic even for such molecules as LnF_3. The covalency of the Ln–X bond increases in the order F → I. The principal contribution to the covalency comes from the Ln 5*d*-, and to a lesser extent, the 6*s*- and 6*p*-orbitals.

Secondly, the majority of LnX_3 in the vapour phase have a pyramidal structure. It is possible that this is a consequence of the participation of 5*d*-orbitals in the chemical bonding. However, a clear link between the pyramidal structure of LnX_3 and the degree of covalency of the Ln–X bond in them has not been established. It is noteworthy that spectral and electron-diffraction investigations are also consistent with a pyramidal structure for LnX_3.[48]

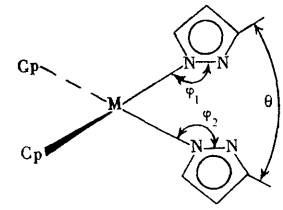
Thirdly, the change of Ln–X bond dissociation energy in LnX_3 correlates with the change of $4f^n6s^2 \rightarrow 4f^{n-1}5d6s^2$ transition energy in the Ln series. This means that the mutual position of the 4*f*- and 5*d*-levels can significantly affect the reactivity of the nascent bond although the 4*f*-orbitals themselves participate little in the bonding.

Fourthly, it is interesting that all calculational methods give results that mainly agree with each other and experiment.

IV. Cyclopentadienyl derivatives of lanthanides and actinides

The most intriguing structural feature of An biscyclopentadienides is that certain $Cp^*_2AnL_2$ [Cp* = pentamethylcyclopentadiene, L = η^2-pyrazolyl (pz), η^2-acyl, etc.] have a 20-electron configuration (considering the total number of valency electrons that is obtained by adding the number of electrons donated by the ligands to the formal number of metals *d*-electrons). However, the majority of transition metal complexes obey the 18-electron rule.[39] Examples of the 20-electron compounds are $Cp^*_2U(\eta^2\text{-pz})_2$,[49] $Cp_2U(acac)_2$,[50] $Cp_2U[O_2C_2CHPMePh_2Fe_2Cp_2(CO)_2]_2$,[51] $Cp^*_2An(\eta^2\text{-COR})_2$ and $Cp^*_2An(\eta^2\text{-CONR}_2)_2$.[52] In particular, the ligands pz^-, COR^- and $CONR_2^-$ can coordinate using one atom (η^1-coordination) or two (η^2-coordination). In the first instance, they act as 2-electron donors; in the second, as 4-electron. The reasons causing such behaviour of the ligands have been analysed in a series of studies.[38,39,53–59] using the quasirelativistic extended Hückel method. In addition, other structural featurs of Th and U biscyclopentadienides were studied.

Three compounds, $Cp_2Mo(pz)_2$, $Cp_2Mo(pz)_2^{2+}$ and $Cp_2U(pz)_2$ (the metal atom in the first molecule has the d^2-electron configuration; in the second d^0), have been examined in order to study the differences in the electronic structure of complexes of *d*-transition metals and Ans.[39] The potential energy surface for these model complexes was calculated as a function of the angles M–N–N and pz–M–pz (angles φ_1, φ_2, and θ).



(I)

The total energy minimum for $Cp_2Mo(pz)_2$ corresponds to the structure with $\eta^1-\eta^1$-coordination of the pyrazoles ($\varphi_1 = \varphi_2 = 128°$, $\theta = 52.5°$). Such structure conforms to the 18-electron rule. The structures with $\eta^1-\eta^2$- and $\eta^2-\eta^2$-coordination of 20- and 22-electron configuration were found to be less stable. On going from the d^2- to the d^0-configuration [i.e., to $Cp_2Mo(pz)_2^{2+}$], the complex with $\eta^1-\eta^2$-coordination becomes more stable. The deficiency of electrons owing to the decreased number of *d*-electrons is reasonably compensated for by η^2-coordination of one of the pz ligands. Thus, the 18-electron rule is again obeyed.

The U complex (in addition to the Th) $Cp_2U(pz)_2$ is ostensibly an analogue of $Cp_2Mo(pz)_2^{2+}$ in the sense that both formally have the d^0-configuration. Nevertheless, the optimal coordination of the pz ligands for them is complete different. Calculations demonstrated that the total energy minimum corresponds to the complex with $\eta^2-\eta^2$-coordination ($\varphi_1 = \varphi_2 = 73°$, $\theta = 113°$). The surprising agreement of these results with the X-ray structure ($\varphi_1 = 75.4°$, $\varphi_2 = 75.1°$ and $\theta = 112.2°$) should be noted.

The geometric structure of these complexes can be understood by analysing the interaction of the frontier orbitals of the fragments. There are three low-energy *d*- and *sp*-hybrid orbitals in the Cp_2Mo^{2+} fragment (Fig. 3*a*). These are the $2a_1$, b_2, and $1a_1$ orbitals. Each pz^- ligand has two orbitals occupied by unshared electron pairs of the N atoms (Fig. 3*b*).

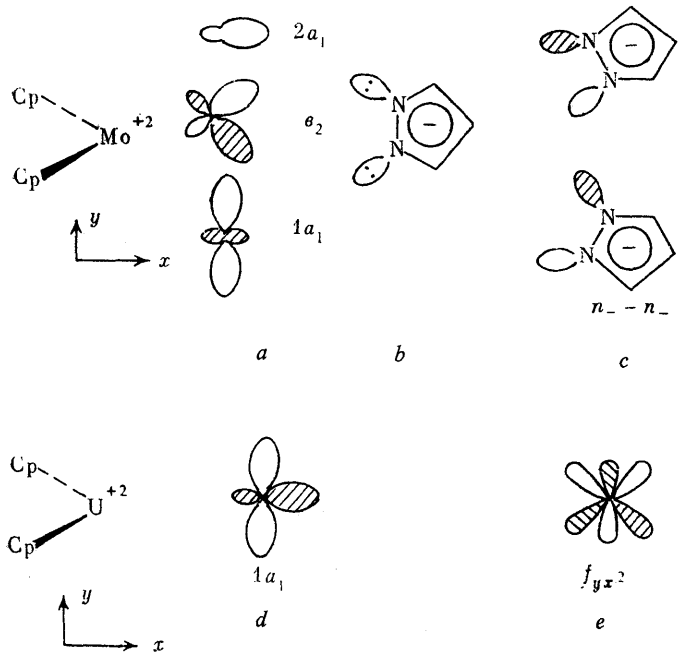


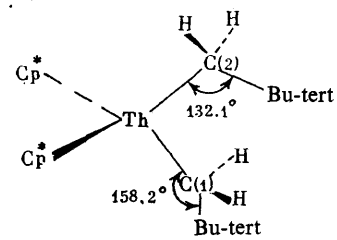
Figure 3. Structure of frontier orbitals of fragments in $cp_2M(pz)_2$ (M = Mo, U). For explanation, see the text.

For the d^2-configuration of Mo, the vacant $2a_1$- and b_2-orbitals of the Cp_2Mo^{2+} fragment interact with one orbital of each pz^- ligand forming the $\eta^1-\eta^1$-coordination. The filled $1a_1$ orbital does not participate in the bonding. For the d^0-configuration, the $1a_1$-orbital can also participate in the bonding. As a result, the structure with $\eta^1-\eta^2$-coordination becomes energetically favorable. The structure with $\eta^2-\eta^2$-coordination always remains energetically unfavorable since the orbitals of the Cp_2Mo^{2+} fragment interact (overlap) poorly with the $(n_- - n_-)$-orbital (Fig. 3*c*), which forms if two pz^- ligands are simulaneously η^2-coordinated.

The Cp_2U^{2+} fragment also has vacant $2a_1$-, b_2- and $1a_1$-orbitals. However, they lie at much higher energy and are more diffuse than the frontier orbitals of Cp_2Mo^{2+}. The shape of the $1a_1$-orbital of Cp_2U^{2+} is different (Fig. 3*d*) from that of Cp_2Mo^{2+}. The components of this orbital for Cp_2U^{2+} along the *x* and *y* axes are about equal whereas the $1a_1$-orbital in Cp_2Mo^{2+} has a shape very close to the pure d_{z^2}-atomic orbital. Another feature is the presence of a vacant f_{yx^2}-orbital for U (Fig. 3*e*) that has the proper symmetry for good overlap with the $(n_- - n_-)$-orbital of two pz^- ligands. Taken together, these features cause the total energy minimum to correspond (i.e., to be energetically favorable) to the $Cp_2U(pz)_2$ complex with $\eta^2-\eta^2$-coordination.

It was also found that these differences in the frontier orbitals affect the structure of $Cp_2M(COR)_2$ and $Cp_2M(CONR_2)_2$, where M = Ti and U.[39,54,56–58] A search for the total energy minimum demonstrated that $\eta^2-\eta^2$-coordination is energetically favorable for M = U whereas $\eta^1-\eta^2$-coordination occurs for M = Ti. In this instance, interaction between donor orbitals of the acyl groups (RC=O) and *f*-orbitals of the An significantly stabilise $\eta^2-\eta^2$-coordination. It is noteworthy that these conditions were also fruitful in understanding the unique reactivity of η^2-coordinated acyl ligands in biscyclopentadienides that is due to the presence of low-lying (in energy) carbene-like acceptor orbitals.[39,57]

The effect of Cp_2An^{2+} (where An = Th) frontier orbitals is evident in the unusual structure of $Cp_2Th(CH_2Bu\text{-}tert)_2$ (II). According to neutron-diffraction data, the angle Th–C(1)–C(alkyl) is 158.2° whereas the other analogous angle Th–C(2)–C is 132.1°.[39,60]



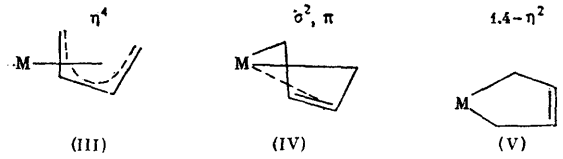
(II)

The quasirelativistic extended Hückel method has been used[39,59] to calculate the potential energy curve for rotation of the ethyl group in Cp_2ThEt_2. The curve was found to be very gently sloped with a shallow minimum at $\alpha = 160°$. An analysis demonstrated that the ethyl group remains strongly bound to the Th in spite of the large deformation (large α). The calculated populations of the overlapping orbitals of the perturbed ethyl group forming the Th–C bond are even slightly greater than those of the unperturbed one. This agrees with the experimentally observed geometric structure of $Cp_2Th(CH_2\text{-}tert)_2$.

Other interesting examples demonstrating the influence of electronic structure on geometric structure are the 1,3-diene complexes $Cp_2M(C_4H_6)$ (where M = Zr and Th). The diene $Cp_2Zr(C_4H_6)$ is known to be able to adopt both the *s-cis*- and *s-trans*-configurations. For example, two geometric isomers of $Cp_2Zr(C_4H_6)$ coexist in solution at 25 °C in the ratio *s-cis*/*s-trans* = 55/45.[61] The *trans* structure becomes more preferred if the terminal

H atoms are replaced by Me- or Ph-groups. The dienes in the isolated An complexes $Cp^*_2Th(C_4H_6)$, $Cp^*_2U(C_4H_6)$, $Cp^*_2Th(CH_2.CMeCMeCH_2)$ and $Cp^*_2Th(CPhHCHCHCPhH)$ have exclusively the *s-cis*-configuration.[38,62,63] Furthermore, whereas low-temperature irradiation of $Cp_2M(s\text{-}cis\text{-}C_4H_6)$ (M = Zr and Hf) leads to formation of the *trans* complexes, such *cis*–*trans* isomerisation is not observed for the analogous Th complex.

The ligand *cis*-butadiene can in principle be bonded to the metal in various ways: by η^4- (III); σ^2,π- (IV); and 1,4-η^2-coordination (V).



(III) (IV) (V)

For example, η^4-coordination is found in $Fe(CO)_3(C_4H_6)$ whereas σ^2,π-coordination (IV) is dominant in complexes of Group IV and V metals. According to X-ray structure analysis, σ^2,π-coordination occurs in Th complexes of butadiene.

Factors determining the preference of butadiene for *s-cis*-coordination in $Cp_2An(C_4H_6)$ (An = U and Th) have been investigated.[38] The total energies of the isomeric forms of the model An complexes $Cp_2An(s\text{-}cis\text{-}C_4H_6)$ (Fig. 4*a*) and $Cp_2An(s\text{-}trans\text{-}C_4H_6)$ (Fig. 4*b*) as functions of the variables *L*, θ and φ were calculated by the quasirelativistic extended Hückel method.

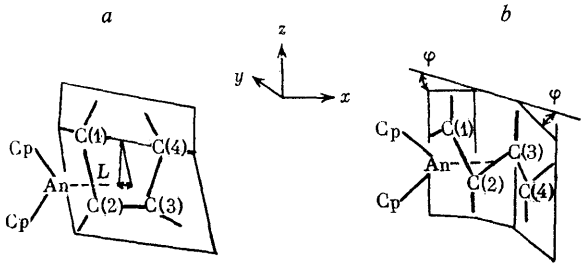


Figure 4. Structure of two isomeric $Cp_2An(C_4H_6)$: *s-cis* (*a*) and *s-trans* (*b*).[38] The variable describes the movement of butadiene as a whole along the *x* axis. The angle θ describes rotation of the molecule around the axis passing through atoms C(1) and C(4). The variable φ (only for the *trans* isomer) characterises the synchronous movement of the two terminal methyl groups toward the metal.

It was found that *s-cis*-coordination is in fact energetically more favourable in the An complex. The corresponding ΔE is 0.74 eV for $Cp_2Th(C_4H_6)$ and 0.42 V for $Cp_2U(C_4H_6)$. The values *L* and θ for the equilibrium structure are consistent with σ^2,π-coordination of *cis*-butadiene to the An. The experimental data are also consistent with this structure. Calculations for the Zr complexes[38,64] indicate that the total energy for $Cp_2Zr(s\text{-}cis\text{-}C_4H_6)$ is more favourable by 0.07 eV than that for $Cp_2Zr(s\text{-}trans\text{-}C_4H_6)$. As in the examples examined above, such a difference between the An and Zr complexes is due to the difference in the structure of the frontier $1a_1$-orbital of Cp_2M^{2+} (M = Zr, U and Th) in addition to the participation of U and Th 5*f*-orbitals in the bonding.

The butadiene molecule has four π-orbitals (π_1, π_2, π_3^*, π_4^*). It has been demonstrated[38] that the bonding Th–π_3^*MO in $Cp_2Th(s\text{-}cis\text{-}C_4H_6)$ contains contributions from the *d*- (16%) and *f*-orbitals (17%) of Th. These orbitals also contribute to the Th–π_2MO at 13 and 2% respectively. Uranium bonds to butadiene in an analogous manner, but there is a slight difference. In the U complex, the 5*f*-orbitals are more involved in the bonding whereas the contribution from the *d*-orbitals decreases. Thus, the bonding U–π_3^*MO is composed of 6 and 48% of U *d*- and *f*-orbitals, respectively.[38]

An important feature of the electronic structure of $Cp_2Th(s\text{-}cis\text{-}C_4H_6)$ is the greater overlap between Th and the terminal C(1) compared with that of the Th–C(2) bond (Table 3). This population difference (ΔP) can serve as an index indicating the preference for one mode of diene coordination or another. The data of Table 3 clearly show that the diene has σ^2,π-coordination in $Cp_2Th(s\text{-}cis\text{-}C_4H_6)$. The value ΔP decreases little on going from Zr to Th. However, it remains larger in both cases than in $Fe(CO)_3(C_4H_6)$. This agrees with experimental data indicating that η^4-coordination occurs in $Fe(CO)_3(C_4H_6)$.

For *s-trans*-coordination, the interaction Th–π_3^* is weaker and the energy level of this orbital is 0.23 eV higher than for $Cp_2Th(s\text{-}cis\text{-}C_4H_6)$. This is the reason for the relative instability of $Cp_2Th(s\text{-}trans\text{-}C_4H_6)$.

In contrast with the An complexes, the interactions Zr–π_3^* in $Cp_2Zr(s\text{-}cis\text{-}C_4H_6)$ and $Cp_2Zr(s\text{-}trans\text{-}C_4H_6)$ are approximately equal. This determines the approximate equal total energies of these complexes.

The electronic structure of U biscyclopentadienides with other ligands is also interesting. Calculations for Cp_2UMe_2 and Cp_2UCl_2 by the $X\alpha$-SW method with relatistic corrections[65] demonstrated that the U 5*f*- and 6*d*-orbitals contribute noticeably to the U–Cp bonds. It was found that the highest occupied molecular orbital in both complexes has almost pure 5*f*-character. The ionisation potentials calculated using the transition-state formalism agree well with expermental data even when spin–orbit coupling is ignored.

Photoelectron spectra of gaseous complexes Cp_2UL_2 (L = BH_4, NEt_2, OCBu-tert, S_2CNEt_2) have been investigated.[66] It was found that the first ionisation potential always correspond to removal of *f*-electrons. For L = NEt_2, the next occupied (after the 5*f*-orbitals) MO is almost purely the atomic 2*p*-orbital of N (with an unshared electron pair). For the other compounds, the next occupied MO is the π-orbital of the Cp ligands. Such a result is consistent with the high reactivity of amidocomplexes relative, for example, to molecules containing polar double bonds and with the smaller lability of the U–Cp bonds in this complex compared with other Cp_2UL_2 complexes.

Data also exist for the electronic structure of Ln biscyclopentadienides. The electronic structure and the nature of the chemical bonding in $Cp_2LuCl.OC_4H_8$ have been studied by the INDO method.[67] The bonds in this complex were found to be covalent. Thus, the bond order (according to Mulliken) Lu–Cl, Lu–O and Lu–C are 0.656, 0.314 and 0.254, respectively (Table 4). The charge on Lu is +0.542. This is far from the +3 predicted by the ionic model. The overlap between the 4*f*- and other orbitals is zero. This means that the 4*f*-orbitals in the complex remain essentially atomic. The overlap data for various orbitals (Table 4) confirm that the 5*d*-orbitals of Lu play a dominant role in the bonding.

Table 3. Electronic population of bonds (P) and atomic charges (Q) in $Cp_2M(s\text{-}cis\text{-}C_4H_6)$, $Cp_2M(s\text{-}trans\text{-}C_4H_6)$ (M = Zr, Th, U) and $Fe(CO)_3(C_4H_6)$.[38]

Compound	P(M—C(1))	P(M—C(2))	ΔP*	Q(C(1))	Q(C(2))
			s-cis		
$Cp_2Zr(C_4H_6)$	0.338	0.060	0.278	−0.100	0.120
$Cp_2Th(C_4H_6)$	0.318	0.049	0.269	−0.398	−0.087
$Cp_2U(C_4H_6)$	0.262	0.029	0.239	−0.282	−0.039
$Fe(CO)_3(C_4H_6)$	0.202	0.184	0.018	−0.220	0.018
			s-trans		
$Cp_2Zr(C_4H_6)$	0.204	0.164	0.040	−0.029	0.072
$Cp_2Th(C_4H_6)$	0.184	0.095	0.089	−0.443	−0.080
$Cp_2U(C_4H_6)$	0.128	0.078	0.050	−0.293	0.072

* ΔP=P(M—C(1)) − P(M—C(2)).

Table 4. Electronic population of orbitals and bonds in $Cp_2LuCl.OC_4H_8$.[67]

Ligand	Orbital	Lu electronic population 6s	6p	5d	4f	Lu–L Bond order
				Orbital population		
–	–	0.377	0.629	1.452	14.000	
				Overlap population		
Cl	3s	0.099	0.207	0.058	0.000	0.656 (Lu–Cl)
	3p	0.036	0.059	0.098	0.000	
O	2s	0.048	0.066	0.064	0.000	0.314 (Lu–O)
	2p	0.011	0.012	0.113	0.000	
C	2s	0.037	0.079	0.020	0.000	0.254 (Lu–C)
	2p	0.018	0.021	0.079	0.000	

The nature of the bonding in Cp_2Ln (Ln = Sm, Eu, Yb) has been studied by comparing photoelectron spectra and quasirelativistic calculations by the $X\alpha$-SW method.[68] An analysis of the MOs revealed that the metal–ring bond is slightly covalent. The small ligand splitting of the 4f-orbitals and their strict localisation are evidence of the ionic interaction. The MOs in Cp_2Eu are ordered the same as in Cp_2Yb. This means that the 4f-levels of divalent Lns do not change their position relative to the energy levels of ligand valence orbitals. This is in contrast with results for LnX_3, where the position of the 4f-orbital energy levels (relative to those of the ligand valence orbitals) depends significantly on the nature of the ligand. The calculated ionisation potentials agree well with the experimental values.

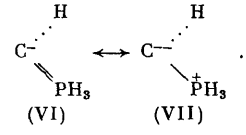
The nature of the bonding of two $LnCp_2$ fragments through H bridges has been studied by the quasirelativistic extended Hückel method.[69] The Ln d-orbitals (in the electronic configuration d^0f^n) apparently stabilise the bridging H atoms. Bonding through symmetric H bridges is energetically more favorable compared with asymmetric bridges.

Besides An biscyclopentadienides, complexes with three cyclopentadienide ligands Cp_3AnL frequently form (in contrast with d-transition metals). The majority of known complexes contain a monodentate anionic ligand (L) such as halide or alkyl and have a trigonal-pyramidal or pseudotetragonal structure. An interesting feature of the Cp_3U fragments is the fact that they can be bonded to η^2-acyl, η^2-pyrazolyl and even η^5-cyclopentadienide ligands in spite of seemingly large steric hindrances to coordination of the last.

The electronic structure of tris(η^5-cyclopentadienyl)An complexes has been studied by the quasirelativistic extended Hückel method.[70,71] Two ligand orbitals in the Cp_3U fragment (C_{3v} symmetry) have a_2 symmetry and can interact only with U $f_{y(3x^2-y^2)}$-orbitals. This means that the f-orbitals can play a significant role in stabilising the An–Cp bond in Cp_3An complexes. Nevertheless, the calculations suggest that the contribution of the $f_{y(3x^2-y^2)}$-orbital to the bonding MO a_2 is amll and reaches only 5–8%. The remaining f-orbitals are essentially nonbonding. The U 6d-, 7s- and 7p-orbitals also participate very little in the bonding. As a result, the population (according to Mulliken) of the U–C(Cp) bonds is very small and reaches only 0.05. Taking into account contributions from H atoms of the C_5H_5 groups, the total overlap U–Cp decreases to 0.01. This contrasts with the high population of M–Cp bonds in transition metal complexes. For example, this value for $CpFeMe(CO)_2$ is 0.57. The small population of the U–Cp bonds indicates that this bond is very weakly covalent and much weaker than the Fe–Cp bond.

Examination of the model complex Cp_3UMe enabled the nature of the σ-bond in An complexes to be analysed. The methyl σ-orbital overlaps mainly with the $6a_1$-orbital (consisting primarily of the U $6d_{z^2}$-orbital) of the CpU fragment. Two other orbitals of the fragment, $3a_1$ and $4a_1$, make a smaller contribution to the bonding interaction. The last two orbitals are primarily f_{z^3} in character. A strong covalent bond between U and Me forms owing to such interactions. The covalent nature of the bonding is consistent with the large overlap of 0.40 in the U–C(Me) bond. It is noteworthy that the corresponding value is 0.44 for the Fe–C(Me) bond in $CpFe(Me)(CO)_2$. The U 7s- (2%), 7p_z- (6%), 6d_{z^2}- (4%) and 5f_{z^3}-orbitals (4%) participate in forming the strong U–C(Me) σ-bond. The contribution of each orbital is small but the sum is 16%.

The nature of the bonding in $Cp_3UCHPPhMe_2$ is of great interest. The anionic ylide ligand can be assigned two resonance forms

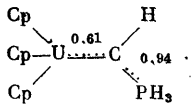


(VI) (VII)

Structure (VII) is formally a dianionic ligand, analogous to a carbene. Hence, U–C double bond can form on coordination of the ylide to U. Quantum-chemical calculations (quasirelativistic extended Hückel method) of the simplified model Cp_3UCHPH_3 demonstrated that the ligand $CHPH_3^-$ has two occupied frontier orbitals. These are a π-orbital with energy −11.3 eV and a σ-orbital with energy −11.9 eV.



Interaction of the σ-orbital with vacant $6a_1$-, $4a_1$-, and $3a_1$-orbitals of Cp_3U^+ forms σ-bonding MO. Furthermore, interaction of the π-orbital with the 8*e*-, 5*e*- and 4*e*-orbitals of Cp_3U^+ forms a π-bonding MO. It should be noted that the 5*e*- and 4*e*-orbitals have primarily f_{yz^2} character. The double bond formed is not localised but has a π-delocalised character U⋯C⋯P:



Nevertheless, the population of the U–C bond is 0.61 (the contribution from the π-component is 0.19). This surpasses the population in other complexes. In general, the calculations demonstrated that the population of the U–C bond in various complexes decreases in the order $Cp_3UCHPH_3 \simeq Cp_3U(C{\equiv}CH) > Cp_3UCH_3 > CpU[CH_2CH_2PH_2]_3$. This correlates with the increasing U–C bond length in this order.

Additional and more accurate data on the electronic structure of tris(cyclopentadienyl)An complexes have been obtained using quasirelativistic *X*α-SW calculations.[72–76] The complexes Cp_3U and Cp_3Th were examined. It was confirmed that the U *f*-orbitals can play an important role in the bonding. It was demonstrated that the U–Cp bond forms through donation of electron density from the π_2-orbital of the Cp ligand into the U 6*d*- and $5f_{y(3x^2-y^2)}$-orbitals. It was found that the highest occupied orbital in Cp_3Th has primarily $6d_{z^2}$ character (89%) and is located 1 eV below the 5*f*-orbitals. The energy level of the 5*f*-orbitals decreases along the series Th → Pu. At the end of the series, it is below the level of the 6*d*-orbitals.

Analysis of the electronic structure of Cp_3UL (where L = H, CO, NO, OH) demonstrated that mainly the U $6d_{z^2}$-orbital participates in bonding to the σ-ligands. The 5*f*-orbitals are not additionally split (compared with Cp_3U). Thus, the bonding orbital for Cp_3UH is 56% hydride in character with the principal contribution coming from the U $6d_{z^2}$-orbital (24%) and small contributions from the $5f_{z^3}$- (1%), 7*s*- (3%) and $7p_z$-orbitals (3%). It must be noted that the relative contribution of the 5*f*-orbitals is greater than the shorter the U–H bond. However, the role of the 6*d*-orbitals in chemical bond formation remains dominant.[74] The contribution of the σ-component remains substantial for Cp_3U complexes with both π-acids (CO, NO) and π-bases (OH). Besides the σ-bonding, π-backbonding occurs in which electrons are donated from the U *f*π-levels into the CO and NO π*-orbitals. Thus, interaction of the CO 2*p*-orbitals with U 5*f*-orbitals in Cp_3UCO forms a bonding orbital consisting of 14% CO orbitals and 84% U orbitals. Such an interaction stabilises the U 5*f*-levels. As with carbonyl complexes of *d*-transition metals, backbonding into a CO antibonding orbital decreases the vibrational frequency of the CO double bond compared with ν_{CO} of the free molecule.

The electronic structure of Cp_3UX (X = F, Cl, Br) has been investigated theoretically (nonrelatistivic *X*α-DV calculations) and experimentally (photoelectron spectra using He I and He II excitation sources).[77] The calculated ionisation potentials for the high (in energy) MOs of Cp_3UCl agree with the experimental values. The conclusion was made that the nonrelativistic calculation can give a good analysis of the photoelectron spectra and an adequate description of the nature of the bonding in An complexes. Nevertheless, the nonrelativistic approach underestimates the contribution of the 6*d*-orbitals (relative to the 5*f*) in forming the metal–ligand bonds. Therefore, a relativistic calculation is required for more accurate information.

Therefore, the following conclusions can be made in finishing this section. Firstly, many of the structural features of An (Th and U) cyclopentadienides, for example, the stability of complexes with a 20-electron configuration, the highly favourable energy of $Cp_2An(s\text{-}cis\text{-}C_4H_6)$ compared with its *trans* isomer, and the unusual geometry of the $Cp_2Th(CH_2Bu\text{-}tert)_2$ structure, are due to participation of both An 6*d*- and 5*f*-orbitals in the chemical bonding.

Secondly, the Ln 4*f*-orbitals in the cyclopentadienides remain essentially atomic. The 5*d*-orbitals play the dominant role in bond formation.

Thirdly, the metal–ligand bonds in Ln and especially in An complexes are not purely ionic but have a significant covalent character.

Application of the quasirelativistic extended Hückel method enables many features of the electronic and geometric structure of cyclopentadienides to be understood qualitatively (and sometimes quantitatively). However, more complicated calculations must be used to obtain more accurate and reliable information on the details of the electronic structure.

Table 5. Electronic population of orbitals and charges on atoms in $M(BH_4)_4$ (M = Zr, U).[85]

A. $Zr(BH_4)_4$

Atom	Charge	Orbital	Population
Zr	+2.02	4*d*	1.95
		4*f*	0.00
		5*s*	0.04
B	−0.50	2*s*	0.89
		2*p*	2.61
H_t	+0.08	1*s*	0.92
H_b	−0.03	1*s*	1.03

B. $U(BH_4)_4$

Atom	Charge	Orbital	Population
Nonrelativistic approximation			
U	+1.93	6*d*	1.11
		5*f*	3.27
		7*s*	−0.11
		7*p*	−0.18
B	−0.42	2*s*	0.88
		2*p*	2.55
H_t	+0.05	1*s*	0.95
H_b	−0.04	1*s*	1.04
Relativistic approximation*			
U	+2.25	6*d*	1.30 (0.56 for $j=3/2$ and 0.74 for $j=5/2$)
		5*f*	2.43 (1.83 for $j=5/2$ and 0.60 for $j=7/2$)
		7*s*	0.11
		7*p*	−0.12 (−0.01 for $j=1/2$ and 0.11 for $j=3/2$)
B	−0.58	2*s*	0.98
		2*p*	2.60 (0.88 for $j=1/2$ and 1.72 for $j=3/2$)
H_t	+0.09	1*s*	0.91
H_b	−0.02	1*s*	1.02

* $j=l+1/2$.

V. Other *f*-element compounds

The electronic structure of uranocene $U(C_8H_8)_2$, which has been investigated in sufficient detail, should be discussed. Calculations have been performed for this molecule using the relatistically parametrised Hückel method,[32] $X\alpha$ (nonrelativistic and relativistic) method.[78–81] and the nonempirical SCF MO method including spin–orbit coupling and a relativistic core potential. In general, results of all these studies agree. It has been found[78–80] that both 5*f*- and 6*d*-orbitals of the metal participate in bonding to the ring. Chang and Pitzer[82] emphasise that the 6*d*-orbitals play the principal role in the covalent bonding; the 5*f*-orbitals, a secondary role. It was also demonstrated that the electronic ground state of uranocene is E_{3g} and the characteristic green colour of uranocene is due to transitions to E_{2u} and E_{3u} excited states. In agreement with the compositions of the MOs, these transitions are qualitatively described as $5f \rightarrow 6d$-transitions.

Of other metallocenes, $Th(C_8H_8)_2$ and $Ce(C_8H_8)_2$ have been investigated.[78,79] The bonding in cerocene was found to be less covalent (more ionic) than in uranocene and thorocene. A study of the photoelectron spectrum also confirms the high covalency of thorocene.[83]

Relativistic and nonrelativistic $X\alpha$-DV methods have been used to study the electronic structure of the borohydrides $M(BH_4)_4$ (M = Zr, U). The results obtained agree with calculations by the $X\alpha$-method.[85] The calculated and experimental ionisation potentials were in good agreement. The relativistic solution better describes the metal–ligand bonding in the U complex. It was demonstrated that the contribution from U 5*f*-orbitals is overestimated and that of the 6*d*-orbitals underestimated in the nonrelativistic approach (Table 5).

Structures of the two η^6-arene complexes $Sm(C_6Me_6)(AlCl_4)_3$ and $U(C_6Me_6)(AlCl_4)_3$ have been compared.[86] The differences in metal–ligand bond lengths was found to be determined by the difference in the U and Sm ionic radii. According to the authors, this means that the acceptor orbitals in the An and Ln complexes are comparable and, therefore, the *f*-orbitals are not involved in bonding to the arene.

Calculations have been performed using the $X\alpha$-SW method for $Eu(C_2H_4)_2$ assuming C_{2v} symmetry.[87] The calculations demonstrated that the complex is weakly bonding owing to donation of charge density from the doubly occupied $f_{z(x^2-y^2)}$-orbital of Eu into the π^*-orbitals of ethylene. However, little density is directly donated from filled ethylene orbitals onto the metal.

A rather large number of molecules and clusters containing 4*f*- and 5*f*-elements has been calculated by the relativistically parametrised extended Hückel method. Reviews of the results have been published.[7,32–35,88] It was demonstrated that this method qualitatively correctly estimates the spin–orbit splitting energies of the valence levels and the role of relativistic effects in the chemical bonding. In particular, it is emphasised[88] that the early 5*f*-elements can be treated as 6*p*-elements in the sense that the 6*p* atomic orbitals of these elements are mixed with ligand orbitals.[7,89] This mixing is especially large in uranyl and other actinyls. Direct experimental proof of the mixing of U 6*p*-orbitals with O 2*p*-orbitals in uranyl and other compounds has been given.[90,91] The contribution of 6*p*-orbitals to nuclear quadrupole coupling has been interpreted on the basis of these results.[35,88]

The electronic structures (quasirelativistic extended Hückel method) of $C_4H_7NdCl_2$. $C_4H_7NdCl_2.3THF$ (THF = tetrahydrofuran) and $C_4H_7Nd(AlCl_4)_2$ (Fig. 5) have been analysed.[92–94] These compounds model the active polymerisation centres of butadiene in the Nd–Al catalytic system. Data for the electronic structure of the *anti*- and *syn*-forms of $C_4H_7NdCl_2$ are presented in Table 6. It was found that the contribution of Nd 4*f*-orbitals to the covalent bonding is insignificant. The partial covalency of the Nd–C bond is due mainly to participation of Nd 5*d*-orbitals in the bonding.

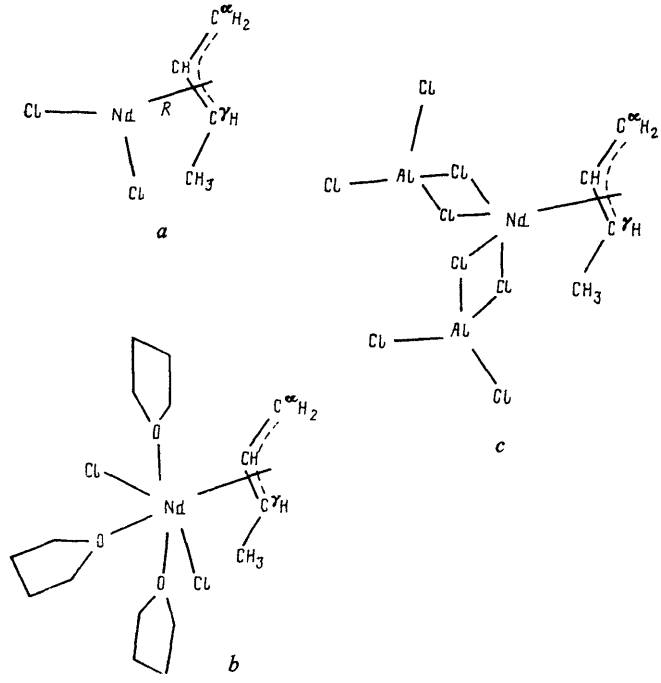


Figure 5. Diagram of active center models, *syn*-$C_4H_7NdCl_2$ (*a*) (*R* is the distance from Nd to the plane of the crotyl group), *syn*-$C_4H_7NdCl_2.3THF$ (*b*), *syn*-$C_4H_7Nd(AlCl_4)_2$ (*c*).

Table 6. Electronic structure of $C_4H_7NdCl_2$ isomers.[93]

$H_{ii}(4f)$, eV	$H_{ii}(5d)$, eV	Isomeric form	ΔE *1	q_i *2				
				$q_{C^{\alpha}}$	$q_{C^{\gamma}}$	q_{Nd}	P (Nd–C^{α}) *3	P (Nd–C^{γ}) *3
−9.82	−8.82	*anti*	10.6	−0.48	−0.33	1.95	0.07(5)	0.08(3)
		syn		−0.45	−0.34	1.93	0.06(5)	0.08(3)
−11.0	−10.8	*anti*	15.5	−0.25	−0.10	0.93	0.12(5)	0.14(4)
		syn		−0.23	−0.11	0.91	0.12(3)	0.16(3)

*$\Delta E = E_{syn} - E_{anti}$, where $E_{syn}(E_{anti})$ is the total energy (kJ mol^{-1}) of the *syn* (*anti*) form; *^2q_i is the excess of electronic charge on the *i*-th atom; *^3P(Nd–C_i) is the electronic population of the Nd–C_i bond. Contributions (%) of partial populations Nd(4*f*)–C_i(2*p*) to the corresponding total populations are given in parentheses.

It was demonstrated that the *syn*-form of the active centres is energetically more favorable than the *anti*-form with respect to the total energy. It was proposed on the basis of the results that kinetic and steric control of the microstructure of polybutadiene is possible in Ln catalytic systems. This validity of this conclusion has been confirmed experimentally.[93,95]

Therefore, existing quantum-chemical methods enable useful information about the electronic and geometric structure of large chemical containing *f*-elements to be obtained. Metal–halide and M–C bonds in these compounds are not purely ionic. The degree of covalency increases on going from Ln to An compounds. The *d*-orbitals of the Lns and Ans make the principal contribution to the chemical bonding. For the latter, the 5*f*-orbitals noticeably participate in forming chemical bonds. This is responsible for many of the strucural features of An compounds. The Ln 4*f*-orbitals interact very weakly with ligand valence orbitals. Their direct contribution to forming chemical bonds is insignificant.

References

1. T J Marks, R D Ernst *Comprehensive Organometallic Chemistry* (Edited by G Wilkinson, F G A Stone, E W Abel), Pergamon Press, Oxford, 1982, Vol. 3, p. 173
2. E F Kustov et al. *Elektronnye Spektry Soedinenii Redkozemel'nikh Elementov* (Electronic Spectra of Rare Earth Compounds), Izd. Nauka, Moscow, 1981, 303 pp
3. V A Gubanov, M V Ryzhkov *Zh. Strukt. Khim.*, 1986, **27** 123
4. V A Gubanov, E Z Kurmaev, A A Ivanitskii *Kvantovaya Khimiya Tverdogo Tela* (Quantum Chemistry of Solids), Izd. Nauka, Moscow, 1984, 304 pp
5. G V Ivanova, V G Pershina, V I Spitsyn *Elektronnoe Stroenie Aktinidov* (Electronic Structure of Actinides), Izd. Nauka, Moscow, 1986, 232 pp
6. G V Ionova *Usp. Khim.*, 1990, **59**(1) 66 [English translation in *Russ. Chem. Rev.*, 1990(1)]
7. P Pyykkö *Chem. Rev.*, 1988, **88** 563
8. K Balasubramanian, K S Pitzer *Adv. Chem. Phys. ab initio Methods in Quantum Chemistry*, Wiley Intersci., 1987, Part 1, Chapter 5, p. 287
9. L Zuelicke *Quantenchemie: Ein Lehrgang, Bd. 1: Grundlagen und Allgemeine Methoden* (Quantum Chemistry: Instruction Course. Vol. 1: Principles and General Methods) (Translated into Russian), Izd. Mir, Moscow, 1976, Vol. 1, 512 pp
10. A Messiah *Quantum Mechanics* (Translated into Russian), Izd. Nauka, Moscow, 1979, Vol. 2, 584 pp
11. A S Davydov *Kvantovaya Mekhanika* (Quantum Mechanics), Izd. Nauka, Moscow, 1973, 704 pp
12. P Pyykko *Adv. Quantum. Chem.*, 1978, **11** 353
13. I B Bersuker *Elektronnoe Stroenie i Svoistva Koordinatsionnykh Soedinenii* (Electronic Structure and Properties of Coordination Compounds), Izd. Khimiya, Leningrad, 1986, 288 pp
14. S R Langhoff, C W Kern *Modern Theoretical Chemistry. Vol. 4. Applications of Electronic Structure Theory* (Edited by H F Schaefer, III), Plenum Press, New York, 1977, Chapter 10, p. 381
15. R McWeeny, B T Sutcliffe *Methods of Molecular Quantum Mechanics* (Translated into Russian), Izd. Mir, Moscow, 1972, 380 pp
16. K Balasubramanian *J. Phys. Chem.*, 1989, **93** 6585
17. *Relativistic Effects in Atoms, Molecules and Solids: Proc. NATO Adv. Study Inst., Vancouver, 10–21 Aug., 1981* (Edited by G L Malli), Plenum Press, New York, 1982, 543 pp
18. *Proceedings of the Symposium on Relativistic Effects in Quantum Chemistry* (Edited by P Pyyko), *Int. J. Quantum Chem.*, 1984, Vol. 25
19. M Krauss, W J Stevens *Annu. Rev. Phys. Chem.*, 1984, **35** 357
20. P A Christiansen, W S Ermler, K S Pitzer *Annu. Rev. Phys. Chem.*, 1985, **36** 407
21. D A Case *Annu. Rev. Phys. Chem.*, 1982, **33** 151
22. K S Pitzer *Int. J. Quantum. Chem.*, 1984, **25** 131
23. L Kahn *Int. J. Quantum. Chem.*, 1984, **25** 149
24. J Slater *Self-consistent Field Methods for Molecules and Solids* (Translated into Russian), Izd. Mir, Moscow, 1978, 663 pp
25. E J Baerends, D E Ellis, P Ross *Chem. Phys.*, 1973, **2** 41
26. K H Johnson *Advances of Quantum Chemistry* (Edited by P-O Lowdin), Acad. Press, New York, 1973, p. 143
27. A Rosen, D E Ellis *Chem. Phys. Lett.*, 1974, **27** 594
28. A Rosen, D E Ellis *J. Chem. Phys.*, 1975, **62** 3069
29. C Y Yang, H-L Yu, D A Case *Chem. Phys. Lett.*, 1981, **81** 170
30. D A Case, C Y Yang *J. Chem. Phys.*, 1980, **72** 3443
31. M Boring, J H Wood *J. Chem. Phys.*, 1979, **71** 32
32. L L Lohr, P Pyykko *Chem. Phys. Lett.*, 1979, **62** 333
33. P Pyykko, L L Lohr *Inorg. Chem.*, 1981, **20** 1950
34. A Viste, M Hotokka, L Laaksonen, P Pyykko *Chem. Phys.*, 1982, **72** 225
35. P Pyykko, L Laaksonen *J. Phys. Chem.*, 1984, **88** 4892
36. S Larsson, P Pyykko *Chem. Phys.*, 1986, **101** 355
37. J P Desclaux *Atomic Data and Nuclear Data Tables*, Acad. Press, New York–London, 1973, Vol. 12, 311 pp
38. K Tatsumi, A Nakamura *J. Am. Chem. Soc.*, 1987, **109** 3195
39. K Tatsumi, A Nakamura *Inorg. Chim. Acta*, 1987, **139** 247
40. A A Bagatur'yants *Itogi Nauki i Tekhniki. T. 14. Kinetika i Kataliz* (Progress in Science and Technology. Vol. 14. Kinetics and Catalysis), Izd. VINITI, Moscow, 1985, 141 pp
41. C E Myers, L J Norman, L M Loew *Inorg. Chem.*, 1977, **17** 1581
42. C F Bender, E R Davidson *J. Inorg. Nucl. Chem.*, 1980, **42** 721
43. B Ruscic, G L Goodman, J Berkowitz *J. Chem. Phys.*, 1983, **78** 5443
44. E Murad, D L Hildenbrand *J. Chem. Phys.*, 1980, **73** 4005
45. L L Lohr, Y Q Jia *Inorg. Chim. Acta*, 1986, **119** 99
46. L-M Li, J-Q Ren, G-X Xu, et al. *Int. J. Quantum Chem.*, 1983, **23** 1305
47. J C Culbertson, P Knappe, N Rosch, M C Zerner *Theor. Chim. Acta*, 1987, **71** 21
48. E Z Zasorin *Zh. Fiz. Khim.*, 1988, **62**(4) 883 [English translation in *Russ. J. Phys. Chem.*, 1988(4)]
49. K G Moloy, T J Marks *Inorg. Chim. Acta*, 1985, **21** 2653
50. C W Eigenbrot, K N Raymond *Inorg. Chem.*, 1982, **21** 2653
51. P J Fagan, J M Manriquez, S H Vollmer, et al. *J. Am. Chem. Soc.*, 1981, **103** 2206
52. R E Cramer, K T Higa, S L Pruskin, J W Gilje *J. Am. Chem. Soc.*, 1983, **105** 6749
53. K Tatsumi, R Hoffmann *Inorg. Chem.*, 1980, **19** 2656
54. K Tatsumi, R Hoffmann *Inorg. Chem.*, 1984, **23** 1633
55. R E Cramer, A T Mori, R B Maynard, et al. *J. Am. Chem. Soc.*, 1984, **106** 5920
56. P Hofmann. P Stauffert, K Tatsumi, et al. *Organometallics*, 1985, **4** 404

57. K Tatsumi, A Nakamura, P Hofmann, et al. *J. Am. Chem. Soc.*, 1985, **107** 4440
58. K Tatsumi, A Nakamura, P Hofmann, et al. *J. Am. Chem. Soc.*, 1986, **108** 4467
59. K Tatsumi, A Nakamura *Organometallics*, 1987, **6** 427
60. J W Bruno, G M Smith, T J Marks, et al. *J. Am. Chem. Soc.*, 1986, **108** 40
61. G Erker, J Wicher, K Engel, et al. *J. Am. Chem. Soc.*, 1980, **102** 6346
62. G M Smith, H Suzuki, D C Sonnenberger, et al. *Organometallics*, 1985, **5** 549
63. G Erker, T Muhlenbernd, R Benn *Organometallics*, 1986, **5** 402
64. K Tatsumi, H Yasuda, A Nakamura *Isr. J. Chem.*, 1983, **23** 145
65. B E Bursten, A Fang *J. Am. Chem. Soc.*, 1983, **105** 6495
66. A L Arduini, J Malito, J Takats, et al. *J. Organomet. Chem.*, 1987, **326** 49
67. L-M Li, J Ren, G-X Xu (K-H Hsu), C Qian *Inorg. Chim. Acta*, 1986, **122** 255
68. J C Green, D Hohl, N Rösch *Organometallics*, 1987, **6** 712
69. J V Ortiz, R Hoffmann *Inorg. Chem.*, 1985, **24** 2095
70. K Tatsumi, A Nakamura *J. Organomet. Chem.*, 1984, **272** 141
71. K Tatsumi, A Nakamura *Applied Quantum Chemistry* (Edited by V H Smith, Jr., H F Shaefer, III, K Morokuma), D Reidel, 1986
72. B E Bursten, R J Strittmatter *J. Am. Chem. Soc.*, 1987, **109** 6608
73. B E Bursten, L F Rhodes, R J Strittmatter *J. Am. Chem. Soc.*, 1989, **111** 2756
74. B E Bursten, L F Rhodes, R J Strittmatter *J. Am. Chem. Soc.*, 1989, **111** 2758
75. B E Bursten, L F Rhodes, R J Strittmatter *J. Less-Common Met.*, 1989, **149** 207
76. R J Strittmatter, B E Bursten *J. Am. Chem. Soc.*, 1991, **113** 552
77. A V Vittadini, M Casarin, D Ajo, et al. *Inorg. Chim. Acta*, 1986, **121** 123
78. N Rösch, A Streitwieser *J. Organomet. Chem.*, 1978, **145** 195
79. N Rösch, A Streitwieser *J. Am. Chem. Soc.*, 1983, **105** 7237
80. N Rösch *Inorg. Chim. Acta*, 1984, **94** 297
81. P M Boerrigter, E J Baerendic, J G Snijders *Chem. Phys.*, 1988, **122** 357
82. A H H Chang, R M Pitzer *J. Am. Chem. Soc.*, 1989, **111** 2500
83. J G Brennan, J C Green, C M Redferm *J. Am. Chem. Soc.*, 1989, **111** 2373
84. D Hohl, N Rösch *Inorg. Chem.*, 1986, **26** 2711
85. D Hohl, D E Ellis, N Rösch, Inorg. Chim. Acta, 1987, **127** 195
86. F A Cotton, W Schwotzer *Organometallics*, 1987, **6** 1275
87. M P Andrews, A L Wayda *Organometallics*, 1988, **7** 743
88. P Pyykko *Inorg. Chim. Acta*, 1987, **139** 243
89. V A Glebov *Elektronnaya Struktura i Svoistva Uranyl'nikh Soedinenii* (Electronic Structure and Properties of Uranyl Compounds), Izd. Energoatomizdat, Moscow, 1983, 88 pp
90. B W Veal, Jr., D J Lam, W T Carnall, H R Hoekstra *Phys. Rev.*, 1976, **12** 5651
91. V P Grechukhin, V I Zhudov, A G Zelenkov, et al. *Pis'ma Zh. Eksp. Teor. Fiz.*, 1980, **31** 627
92. Z M Sabirov, Yu B Monakov *Dokl. Akad. Nauk SSSR*, 1988, **302** 143
93. Z M Sabirov, Yu B Monakov, G A Tolstikov *J. Mol. Catal.*, 1989, **56** 194
94. Z M Sabirov, Yu B Monakov *Inorg. Chim. Acta*, 1989, **169** 221
95. Z M Sabirov, N Kh Minchenkova, N A Vakhrusheva, Yu B Monakov *Dokl. Akad. Nauk SSSR*, 1990, **312** 147